



**HAL**  
open science

## In-Can vitrification of ash

Maxime Fournier, Nicolas Massoni, J-Francois F Hollebecque

► **To cite this version:**

Maxime Fournier, Nicolas Massoni, J-Francois F Hollebecque. In-Can vitrification of ash. IOP Conference Series: Materials Science and Engineering, 2020, 818 (1), pp.012005. 10.1088/1757-899X/818/1/012005 . cea-03579858

**HAL Id: cea-03579858**

**<https://cea.hal.science/cea-03579858>**

Submitted on 18 Feb 2022

**HAL** is a multi-disciplinary open access archive for the deposit and dissemination of scientific research documents, whether they are published or not. The documents may come from teaching and research institutions in France or abroad, or from public or private research centers.

L'archive ouverte pluridisciplinaire **HAL**, est destinée au dépôt et à la diffusion de documents scientifiques de niveau recherche, publiés ou non, émanant des établissements d'enseignement et de recherche français ou étrangers, des laboratoires publics ou privés.



Distributed under a Creative Commons Attribution 4.0 International License

# In-Can vitrification of ash

**M Fournier, N Massoni and J F Hollebecque**

CEA, DEN, DE2D, Univ. Montpellier, Marcoule, F-30207 Bagnols-sur-Cèze

maxime.fournier@cea.fr

**Abstract.** The In-Can Melter is a metallic crucible heated in a refractory furnace using electrical resistors allowing in-container vitrification. The In-Can Melter trial aims to demonstrate the feasibility of the confinement in a glassy matrix of ash coming from existing incineration processes. The ash was pelletised to allow its introduction into the can without dust emissions and then incorporated in a 50 wt.% waste loading confinement matrix. The full-scale trial was preceded by laboratory- and bench-scale tests. The microstructure and chemical durability of the wasteform were characterised.

## 1. Introduction

The Thermal treatment for radioactive waste minimisation and hazard reduction (THERAMIN) project is a European Commission programme of work jointly funded by the Horizon 2020 Euratom research and innovation program and various European nuclear waste management organisations (WMOs). The THERAMIN project is being conducted between June 2017 and May 2020. Twelve European WMOs and research and consultancy institutions from seven European countries are participating in THERAMIN. The overall objective of THERAMIN is to provide improved, safe long-term storage and disposal of intermediate-level waste and low-level waste suitable for thermal processing. The work programme provides a vehicle for coordinated European Union-wide research and technology demonstrations designed to provide improved understanding and optimisation of the application of thermal treatment in radioactive waste management programmes across Europe, and moves technologies higher up the Technology Readiness Level (TRL) scale.

In the framework of the THERAMIN project, the French Alternative Energies and Atomic Energy Commission (CEA) carried out studies on the treatment and conditioning of ash resulting from the incineration of technological surrogate waste. The trial described in this article is based on the CEA In-Can Melter (ICM) consisting of a metallic crucible melter heated in a refractory furnace. Prior to the full-scale trial, laboratory- and bench-scale tests were conducted to select optimised operating conditions. Wasteforms produced were characterised after the trials.

## 2. Description of the CEA's In-Can Melter

The ICM is a metallic crucible heated in a refractory furnace using electrical resistors (Figure 1). The can, with an approximate volume of 50 L, is renewed after each filling. The process can support either liquid or solid waste feeds. With the current off-gas treatment system (not including a post-combustion chamber), it can only tolerate small amounts of organics. It can also accept a small fraction of metal in the waste. The design ensures that the process can operate remotely for high-activity waste. The design can also be adapted for dealing with plutonium-containing material in gloveboxes. The end product can be glass, glass ceramic, or simply a high-density waste product.



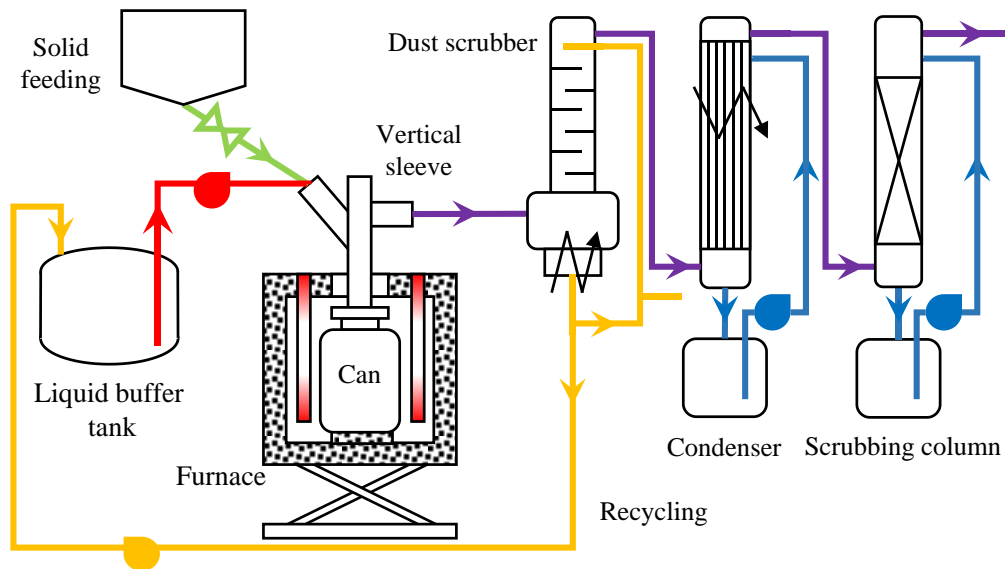


**Figure 1.** Diagram of the CEA’s In-Can Melter.

ICM has been developed for CEA needs since 2005 for military waste vitrification. The technology is at TRL 7 and the ICM has undergone inactive commissioning in France with inactive simulants of alpha effluent. The technology is currently being qualified for solid waste.

### 3. Ash production

The waste selected for this vitrification trial is the ash from multiple incineration tests of surrogate technological waste (polyvinyl chloride, latex, neoprene, polyethylene, cotton, etc.) produced by the CEA’s IRIS process (French acronym for Research facility for solid waste incineration). IRIS is a research facility for the incineration of solids developed to treat organic waste from gloveboxes in the nuclear industry, contaminated with alpha-bearing actinides and containing high quantities of chlorine (Figure 2).

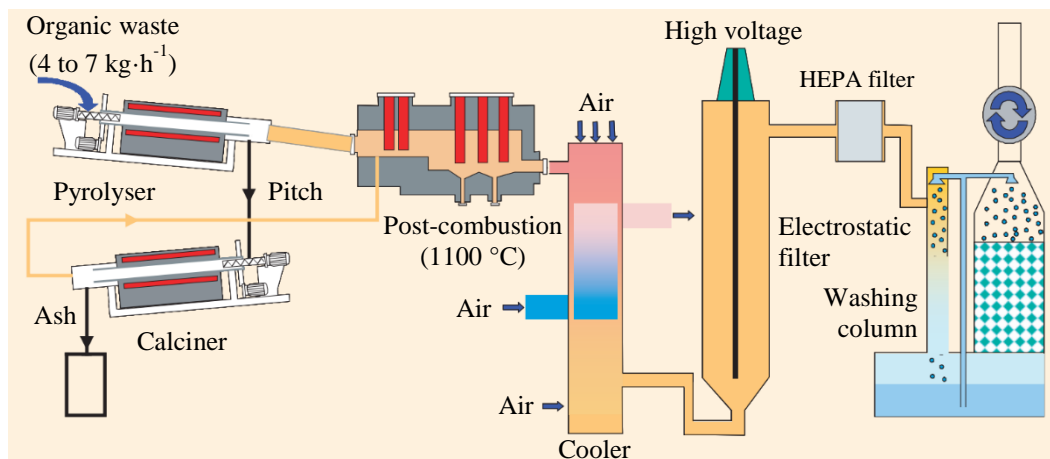


**Figure 2.** Diagram of the CEA’s IRIS process for the treatment of organic waste.

The robustness and efficiency of this process is based on a decoupling of (i) the step of elimination of corrosive materials such as chlorine and (ii) the step of combustion of the organic waste. Figure 2 shows that the organic waste first goes into a pyrolysis step at a temperature of 500 °C to remove the most corrosive gaseous compounds and then into a calciner (900 °C) fed with oxygen to complete the combustion while concentrating the contamination in the mineral ash. The relatively long residence time

in furnaces with low gas flow rates makes it possible to produce carbon-free ash, concentrating almost all of the initial activity. The off-gas treatment system, consisting of a post-combustion chamber followed by electrostatic filtration, ensures excellent purification.

#### 4. Pre-treatment of ash and definition of their vitrification conditions

In order to obtain a sufficient amount of ash to carry out the various tests described thereafter, 230 batches, each containing approximately 220 g of ash from various IRIS trials, were homogenised using a Morton Mixers ribbon blender (Figure 3.a-b). This operation resulted in a decrease in the size of the ash agglomerates, with an ash apparent density of  $0.6 \text{ g}\cdot\text{cm}^{-3}$ , compared to  $0.2 \text{ g}\cdot\text{cm}^{-3}$  before homogenisation, and a true density of  $1.9 \text{ g}\cdot\text{cm}^{-3}$  measured by helium pycnometry. The composition of the ash thus mixed (Table 1) was analysed by X-ray fluorescence spectroscopy (XRF).

Ash is characterised by a high volatility that can lead to clogging of the feeding and off-gas treatment system pipes and large dust carry-over. In order to limit this volatility, a temporary densification by pelletisation was carried out using a Frogerais rotative press. The ash was pressed in the presence of a binder to ensure the mechanical cohesion of the pellets, but without glass frit, being too abrasive for the press. Two types of binder were tested: organic (sorbitol,  $\text{C}_6\text{H}_{14}\text{O}_6$ , or fructose,  $\text{C}_6\text{H}_{12}\text{O}_6$ ) and mineral (bentonite, mainly containing montmorillonite  $(\text{Na,Ca})_{0.33}(\text{Al,Mg})_2\text{Si}_4\text{O}_{10}(\text{OH})_2(\text{H}_2\text{O})_n$ ). The addition of 10 wt.% of fructose or bentonite to the ash gave similar and satisfactory results. Bentonite was preferred thereafter to avoid possible  $\text{CO}_x$  gas emissions during combustion. Approximately 60,000 pellets (9 kg of ash), reaching a 72% densification, were produced (Figure 3.c).



**Figure 3.** Ash in the mixer (a) before and (b) after homogenisation. (c) Ash pellets.

In order to determine the vitrification conditions of the ash, laboratory-scale tests, using small quantities of materials ( $\approx 10 \text{ g}$ ), were carried out with different amounts of ash and glass frit at  $1100 \text{ }^\circ\text{C}$  for 2 h. In the approach proposed in the THERAMIN project, no vitreous matrix formulation study was carried out and FN0C77 glass frit (Table 1), simple and available, was used. At the end of the tests, the crucibles were cut and the materials obtained were observed with a binocular magnifier and evaluated according to two criteria: (i) obtention of a macroscopically homogeneous material and (ii) the absence of foaming during melting. The best results were obtained for a 50:50 mixture between ash and glass frit. Beyond this ratio, the reactivity between ash and glass frit is less efficient and the resulting material becomes less homogeneous.

#### 5. Bench-scale test and characterisation of the wasteform

##### 5.1. Test conditions

Following the laboratory-scale tests, the quantity of treated ash was increased during a bench-scale test. This test was carried out in an Inconel<sup>TM</sup> 601 crucible having an external diameter of 100 mm and a thickness of 5 mm, filled with 400 g of un-pelletised ash and 400 g of FN0C77 glass frit (Figure 4.a).

The tapped density of this mixture was estimated at approximately  $1 \text{ g}\cdot\text{cm}^{-3}$ . The mixture was heated at  $300 \text{ }^\circ\text{C}\cdot\text{h}^{-1}$  and maintained at  $1100 \text{ }^\circ\text{C}$  for 8 h.

At the end of the test (Figure 4.b), the crucible was cut and the resistance of Inconel™ 601 to corrosion was evaluated. No significant corrosion is seen at the interface between Inconel™ and the wasteform. Above the volume occupied by the wasteform, gaseous species superficially corroded the Inconel™ (Figure 4.c). The crystallised corrosion products are  $\text{NiFe}_{1.2}\text{Cr}_{0.8}\text{O}_4$  spinels and nickel oxide. However, no significant reduction in the thickness of the crucible is measured. A mass loss of 2.5 wt.% was measured after the test and a crystallised glass of density  $2.63 \text{ g}\cdot\text{cm}^{-3}$  was obtained (Figure 4.d).

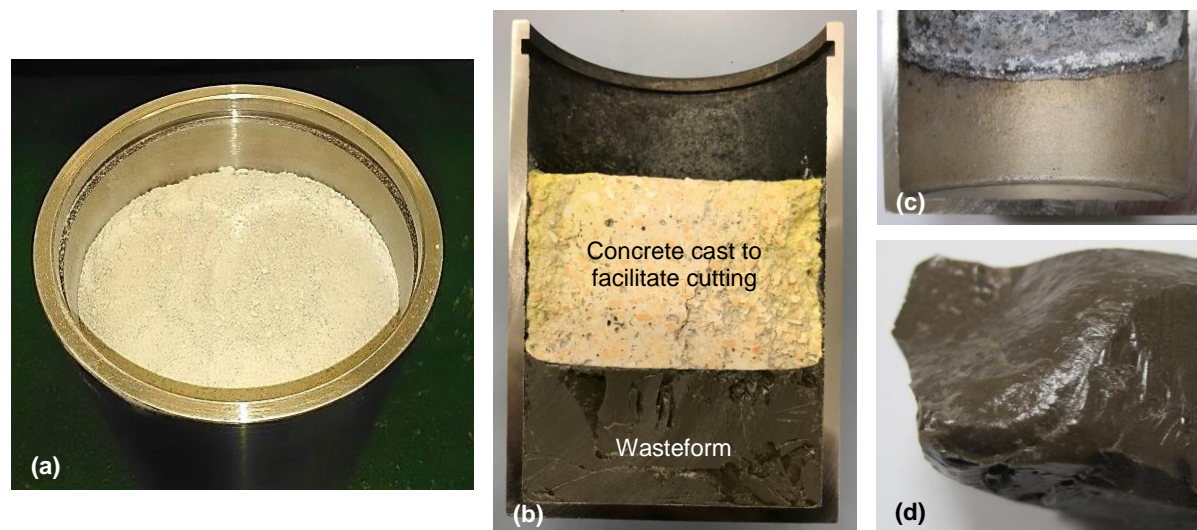


**Figure 4.** (a) Ash and glass frit mixture introduced into the Inconel™ 601 crucible, (b) crucible cut after the test, (c) inner surface of the crucible after the test and (d) wasteform produced.

### 5.2. Microstructure and chemical composition of the wasteform

The material is mainly composed of a vitreous matrix consisting of approximately 80 wt.% of  $\text{Al}_2\text{O}_3$ ,  $\text{B}_2\text{O}_3$ ,  $\text{CaO}$ ,  $\text{Na}_2\text{O}$ , and  $\text{SiO}_2$ . This matrix includes three types of crystallisation identified by scanning electron microscopy (SEM) and X-ray diffraction (XRD): apatites, zincochromites, and beads composed almost exclusively of bismuth (Figure 5 and Table 1). The stoichiometries of apatites and zincochromites evaluated by energy dispersive X-ray spectroscopy (EDS), respectively  $\text{Ca}_{4.8}\text{P}_{2.9}\text{Si}_{0.3}\text{Na}_{0.2}\text{Al}_{0.1}\text{O}_{12.9}$  and  $\text{ZnCr}_{2.6}\text{Na}_{0.5}\text{Mg}_{0.2}\text{Al}_{0.1}\text{Fe}_{0.1}\text{Ni}_{0.1}\text{O}_{5.8}$  (oxygen assumed for stoichiometry), are consistent with the theoretical stoichiometries of these minerals, respectively  $\text{Ca}_5(\text{PO}_4)_3(\text{OH})$  and  $\text{ZnCr}_2\text{O}_4$ . The crystals are homogeneously distributed in the matrix, with the exception of a layer approximately one millimetre thick at the interface with the crucible in which they are more numerous.

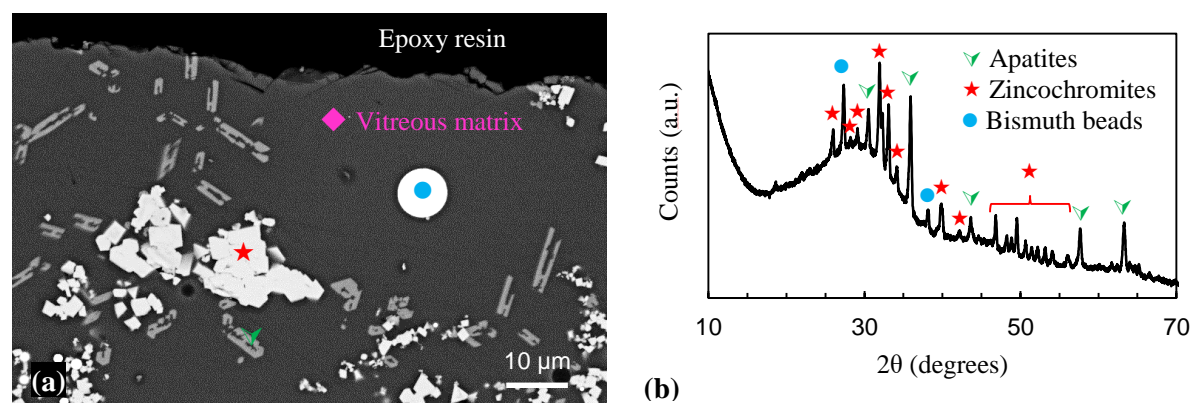


**Figure 5.** (a) SEM and (b) XRD analysis of the wasteform produced at the bench-scale.

**Table 1.** Elemental compositions, expressed in wt.%, of ash and glass frit used for the calculation of the theoretical composition of the wasteform. Analysed compositions of the vitreous and crystalline phases composing the wasteform.

Element	Ash (analysed by XRF)	FN0C77 glass frit (specified)	Wasteform (calculated)	Vitreous matrix (analysed by EDS)	Apatites (analysed by EDS)	Zincochromites (analysed by EDS)	Bismuth beads (analysed by EDS)
Al	11.90		5.95	9.40	0.06	0.15	
B		10.05	5.02	n.a. <sup>a</sup>	n.a. <sup>a</sup>	n.a. <sup>a</sup>	n.a. <sup>a</sup>
Ba	0.71		0.36				
Bi	4.02		2.01	0.17			9.99
Ca	9.91		4.96	7.10	4.84	0.01	
Cl	1.42		0.71		0.08		
Cr	0.12		0.06			2.58	
Fe	0.50		0.25	0.61		0.05	
K	2.25		1.13	1.56			
Mg	1.59		0.80	3.00		0.24	
Na	0.55	23.74	12.14	13.71	0.16	0.48	
Ni	0.69		0.35			0.05	0.17
P	1.62		0.81	0.62	2.88		
S	0.31		0.16	0.32			
Sb	0.15		0.08				
Si	7.45	16.57	12.01	27.71	0.25	0.02	
Ti	0.45		0.23	1.04		0.03	
Zn	8.13		4.07	5.74		1.00	0.25

<sup>a</sup> n.a.: not analysed because boron is not detected by EDS.

### 5.3. Chemical durability

The chemical durability of the material was studied according to a protocol adapted from the PCT-B standardised test [1]. After crushing the material, 125–250  $\mu\text{m}$  of powder were placed in contact with pure water with a glass-surface-area-to-solution-volume ratio ( $S/V$ ) of  $10 \text{ m}^{-1}$  at  $90 \pm 2 \text{ }^\circ\text{C}$  in unstirred perfluoroalkoxy (PFA) reactors. The powder specific surface area of  $259 \text{ g}\cdot\text{cm}^{-2}$  was estimated by adsorption of krypton on the sample surface (Micromeritics ASAP 2020) according to the Brunauer–Emmett–Teller theory [2]. Solution samples, taken at regular intervals, were filtered with a cut-off of  $0.45 \text{ }\mu\text{m}$ , acidified with ultrapure grade  $\text{HNO}_3$  and analysed by inductively coupled plasma-atomic emission spectroscopy (Thermo Scientific iCAP™ 6000 Series). The concentrations were used to calculate normalised mass losses  $\text{NL}_i = C_i / (x_i \times S/V)$ , where  $C_i$  is the concentration of the element  $i$  and  $x_i$  the mass percentage of  $i$  in the glass. The alteration rate,  $r = \text{dNL}_i / \text{dt}$ , was calculated by linear regression. Boron is known to be an alteration tracer of the vitreous matrix, which means that it is not retained in alteration products while released from the glass.

The evolution of the normalised mass losses of Al, B, Na, and Si is shown in Figure 6.a. Only the elements mainly integrated into the vitreous matrix are considered. The  $x_i$  considered are those obtained by EDS analysis for Na, Si, Al, and by calculation for B. Therefore, the dissolution rates of the crystalline phases are not considered, because when a wasteform contains crystalline phases deemed to be durable,

like apatites or spinels, the wastefrom dissolution is controlled by the properties of the vitreous matrix [3]. This leaching test was duplicated, giving similar results: the average values obtained are discussed hereafter.

On the first day of leaching, the alteration rate of the vitreous matrix is  $\geq 2.4 \text{ g}\cdot\text{m}^{-2}\cdot\text{d}^{-1}$ . After 3 days, the rate is  $\approx 1.5 \text{ g}\cdot\text{m}^{-2}\cdot\text{d}^{-1}$ . The alteration therefore decreases over time and quickly becomes non-stoichiometric, showing the typical behaviour of a borosilicate glass of nuclear interest. Si and Al are retained at 30–40% in the alteration layer after one month. Such retention remains relatively low: the amorphous layer formed on the sample surface therefore remains poor in silicon, which explains why the hydrolysis regime remains predominant. The initial dissolution rate of the vitreous matrix leads to a rapid increase in  $\text{pH}_{90^\circ\text{C}}$  to 8.5, the value at which this parameter stabilises.

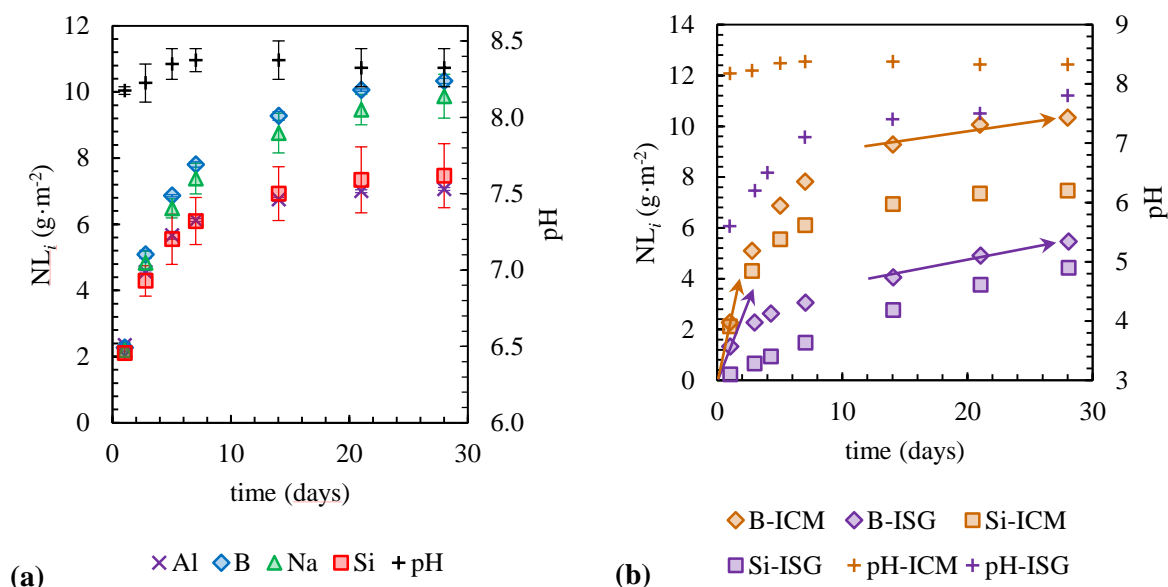


**Figure 6.** (a) Evolution of NL and pH during wastefrom leaching (error bars represent the data dispersion between the duplicates). (b) Compared evolution of NL and pH during the leaching of ISG and In-Can-produced wastefrom. The arrows are a visual guide to estimate the drop in alteration rate.

Comparison of previous results with those acquired for the reference International Simple Glass (ISG) [4, 5] altered under the same conditions (Figure 6.b) shows similar and ‘classical’ trends.

- Because of its composition, the In-Can-produced vitreous matrix has a higher rate of hydrolysis. Indeed, it contains large fractions of  $\text{Na}_2\text{O}$  and  $\text{B}_2\text{O}_3$ , which are unfavourable to the glass durability. Therefore, in the early stages of dissolution, the evolutions of the concentrations in solution are faster for In-Can-produced wastefrom. This conclusion is also valid for the pH evolution.
- The growth of the alteration layer is faster for the In-Can-produced wastefrom. Thus, its alteration rate drops faster. Between 14 and 28 days, the alteration rate of the In-Can-produced vitreous matrix ( $0.07 \text{ g}\cdot\text{m}^{-2}\cdot\text{d}^{-1}$ ) is almost 1.5 time lower than that of the ISG ( $0.10 \text{ g}\cdot\text{m}^{-2}\cdot\text{d}^{-1}$ ), while the hydrolysis rate of the vitreous phase of the wastefrom after 1 day is higher. This result is known for simple glasses [6]: the glasses that are hydrolysed the fastest are also those that have the earliest rate drops.

The data trends tend to show that, in the longer term, an alteration layer will form on the In-Can-produced wastefrom, causing a decrease of the alteration rate, as for the ISG.

## 6. Full-scale trial

A full-scale trial was conducted with the CEA's ICM (Figure 1). The can is made of Inconel™ 601, with an external diameter of 400 mm, a height of 600 mm and a wall thickness of 10 mm.

The trial began with pre-loading of the container with 25 kg of FN0C77 glass frit and 17.8 kg of un-pelleted ash. This mixture was heated at  $300\text{ }^{\circ}\text{C}\cdot\text{h}^{-1}$  up to  $1100\text{ }^{\circ}\text{C}$ . Then, 9.2 kg of pelleted ash were fed into the can with a flow of  $10\text{ kg}\cdot\text{h}^{-1}$ , before the introduction of 1 kg of FN0C77 frit and an additional soaking of 2 h. Thus, the final waste loading was 50 wt.%. The test was continued with 2 h of recycling of the dust recovered in the off-gas treatment system and 2 h of further soaking. The can was then allowed to cool freely. A loss of mass of 2.3 wt.% was measured, consistent with that of the test carried out at bench-scale.

The extent of characterisation of the material produced during this trial is more limited than that of the material produced at bench-scale. However, the SEM and XRD characterisations carried out on a sample taken in the central zone of the can show a similar microstructure (Figure 7). The same bismuth beads, apatite, and zincochromite crystals are included in a vitreous matrix.

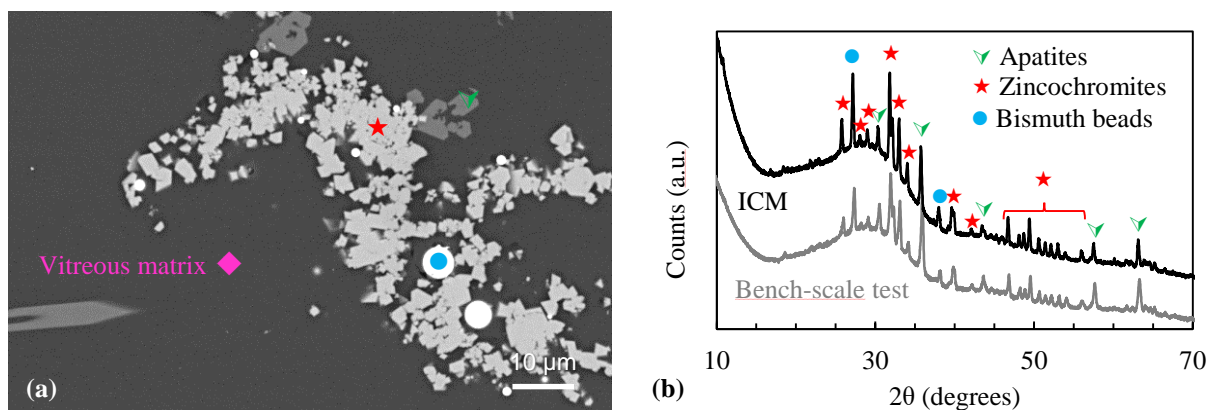


**Figure 7.** (a) SEM image and (b) XRD analysis of the wasteform produced using the ICM. The XRD results are compared to those of the bench-scale test.

## 7. Conclusions

The In-Can Melter trial conducted in the framework of the THERAMIN project demonstrated a successful process for the vitrification of ash generated from the incineration of organic waste from glove boxes in the nuclear industry. This study presents — in a simplified version — the scale up methodology used to demonstrate the feasibility of the thermal treatment of a given waste by a given process. Thus, the laboratory-scale tests assess the waste loading, operating temperature, mixture strategy and melted material quality. Next comes the bench-scale test focusing on crucible corrosion, volatility of some species and wasteform microstructure. Finally, the study concludes with a pilot-scale trial whose main outputs are overall corrosion and kinetic data, process performance, process and package descriptions.

A good waste loading of 50 wt.% was achieved in this first approach. The trial also made it possible to begin the technical investigation required for the processing of powdery solids into the can while avoiding dust emission: a temporary densification by pelletising was implemented.

The produced wasteform consists of a crystallised glass mainly composed of  $\text{SiO}_2$ ,  $\text{Na}_2\text{O}$ ,  $\text{B}_2\text{O}_3$ ,  $\text{Al}_2\text{O}_3$ , and  $\text{CaO}$ . The term ‘crystallised glass’ refers to a vitreous matrix including crystals of apatite, zincochromite, and bismuth alloy. The crystals are distributed homogeneously in the wasteform.

The crystalline phases being durable, the durability of the wasteform is controlled by that of the vitreous matrix. The hydrolysis rate of this glass is relatively high because of its high content of  $\text{B}_2\text{O}_3$  and  $\text{Na}_2\text{O}$ . Indeed, in the approach proposed in the framework of the THERAMIN project, no optimisation study of the glass additives was conducted. However, the ‘classical’ trends observed suggest that, in the long term, an alteration layer will form, leading to a decrease in the alteration rate.

### Acknowledgements

This project has received funding from the Euratom research and training programme 2014–2018 under grant agreement No 755480. This paper reflects only the authors' views, and the European Commission is not responsible for any use that may be made of it.

The authors are grateful to Alain Artico, Carine Castaño, and Virginie Lemaitre for carrying out the tests, Thierry Blisson, Florian Emanuel, and Valérie Debono for the wasteform characterisation, and PRIME Verre Company for its technical assistance.

### References

- [1] ASTM International 2014 *Standard C1285-14. Standard Test Method for Determining Chemical Durability of Nuclear, Hazardous, and Mixed Waste Glasses and Multiphase Glass Ceramics: The Product Consistency Test (PCT)*
- [2] Brunauer S, Emmett P H and Teller E 1938 Adsorption of gases in multimolecular layers *J. Am. Chem. Soc.* **60** 309–19
- [3] Nicoleau E, Angeli F, Schuller S, Charpentier T, Jollivet P and Moskura M 2016 Rare-earth silicate crystallization in borosilicate glasses: Effect on structural and chemical durability properties *J. Non-Cryst. Solids* **438** 37–48
- [4] Gin S, Abdelouas A, Criscenti L J, Ebert W L, Ferrand K, Geisler T, Harrison M T, Inagaki Y, Mitsui S, Mueller K T, Marra J C, Pantano C G, Pierce E M, Ryan J V, Schofield J M, Steefel C I and Vienna J D 2013 An international initiative on long-term behavior of high-level nuclear waste glass *Mater. Today* **16** 243–8
- [5] Kaspar T C, Ryan J V, Pantano C G, Rice J, Trivelpiece C, Hyatt N C, Corkhill C L, Mann C, Hand R J, Kirkham M A, Crawford C L, Jantzen C M, Du J, Lu X, Harrison M T, Cushman C, Linford M R and Smith N J 2019 Physical and optical properties of the International Simple Glass *npj Mater. Degrad.* **3** 15
- [6] Gin S, Beaudoux X, Angéli F, Jégou C and Godon N 2012 Effect of composition on the short-term and long-term dissolution rates of ten borosilicate glasses of increasing complexity from 3 to 30 oxides *J. Non-Cryst. Solids* **358** 2559–70